



## Adsorption of As(III) from aqueous solutions by iron-impregnated quartz, lignite, and silica sand: kinetic study and equilibrium isotherm analysis

Shashi B. Gautam<sup>a</sup>, R.C. Vaishya<sup>b</sup>, G.L. Devnani<sup>a</sup>, Anil K. Mathur<sup>c,\*</sup>

<sup>a</sup>Chemical Engineering Department, Harcourt Butler Technological Institute, Kanpur 208002, India

<sup>b</sup>Civil Engineering Department, Motilal Nehru National Institute of Technology, Allahabad 211004, India

<sup>c</sup>Pollution Control Board, Lucknow 226010, Uttar Pradesh, India

Tel. +91 562 2275014; Fax: +91 562 2275014; email: anilmathur@rediffmail.com

Received 21 December 2011; Accepted 9 April 2013

### ABSTRACT

In this study, adsorption of As(III) removal on iron oxide-coated quartz, iron oxide-coated lignite sand, and iron oxide-coated silica sand were investigated. Batch studies were performed to evaluate the influences of various parameters like initial pH, adsorbent dose, and initial concentration for the removal of As(III). Optimum conditions for As(III) removal on the three adsorbents were found to be pH 7, adsorbent dose 20 g/l of solution, and equilibrium time 6 h. The kinetics study of As(III) removal have also been determined using a pseudo-first-order, pseudo-second-order, Weber and Morris, and Elovich model. Among the conventional models, the  $q_{e,exp}$  and the  $q_{e,calc}$  values from the pseudo-second-order kinetic model are very close to each other and followed by Weber–Morris and Elovich model for all adsorbents. In this system, the effective diffusion coefficient ( $D_e$ ) value of As(III) is more than the order of  $10^{-9}$  cm<sup>2</sup>/s. This order shows in the literature that pore diffusion is the rate-limiting step for all the adsorbents. Equilibrium isotherms for the adsorption of As(III) on all the three adsorbents were analyzed by Langmuir, Freundlich, Redlich–Peterson (R–P), and Temkin isotherm models using nonlinear regression technique. R–P and Freundlich isotherm was found to be the best to represent the data for As(III) adsorption on all the adsorbents. The parameters obtained in this study for different kinetic and equilibrium models of all adsorbents are very comparable with other reported values for sand-based and other adsorbents.

*Keywords:* Adsorption; As(III); IOCLS; IOCQS; IOCSS; Isotherms; Kinetics

### 1. Introduction

Water is one of the prime elements responsible for life on earth. The water contaminated with enormous quantities of heavy metals as pollutants is being

released by various industries because of the broad range of applications of heavy metals among the top chemical compounds used in many industries. Out of many heavy metalloids, arsenic is of major concern as an environmental pollutant due to its recalcitrant and toxic nature [1–5]. Leaching from geological formations is a major natural source of arsenic in

\*Corresponding author.

ground water. Chronic health effects of arsenic include, development of various skin lesions, such as hyper pigmentation dark spots, hypo pigmentation white spots, keratoses, corns, and small warts of the hands and feet. Skin cancers and internal cancers ~lung, kidney, liver, and bladder can appear due to high arsenic exposure [1–4,6]. Humans may be exposed to arsenic mainly through food and water, particularly in certain areas, where the groundwater is in contact with arsenic-containing mineral [1–2,5–7]. Studies have reported that people exposed to high levels of arsenic are having severe health problems in many countries like Argentina, India, Pakistan, Mexico, Germany, Bangladesh, USA, Canada, America, Hungary, Nepal, Myanmar, Cambodia, etc [6–8].

From the Priority List of Hazardous Substances Comprehensive Environmental Response, and Compensation and Liability Act [9], arsenic is ranked first among 275 substances identified to pose the most significant potential threat to human health. Arsenic is also classified as a hazardous substance in the Environmental Protection Agency list of priority pollutants. Considering the lethal impact of arsenic on human health, environmental authorities have taken a more stringent attitude towards the presence of arsenic in water. The World Health Organisation and the United States (USEPA) has set a standard of 10 µg/l [1,10,11]. Australia, Japan, and Canada have recommended a maximum contaminated level of arsenic in drinking water as 7, 10, and 25 µg/l, respectively [10,12]. However, for India, Bangladesh, Taiwan, and Vietnam, this limit is still as high as 50 µg/l [13]. In India, many districts of West Bengal are facing the problem of arsenic contamination of groundwater.

Various physico-chemical methods for the treatment of arsenic contamination have been investigated. These include adsorption [1–7], biodegradation [14–17], and biosorption [14]. Recently, few researchers have reported that the iron oxide-coated sand (IOCS) [1–4,18–20] has very good arsenic removal capacity. In these investigations, a wide range of adsorbent doses have been taken and effects of process parameters (pH, temperature and agitation periods) on the removal of arsenic by IOCS and iron oxide-coated quartz sand (IOCQS) have been reported.

Some work has also reported on the Fe- and Mn-impregnated granulated activated charcoal (GAC-Fe) and the comparable removal of arsenic from water [6,21–26]. Though adsorption of arsenic on iron-coated different sand has been studied by many workers [1–4,18,26], the information available on analysis of kinetics and equilibrium parameters are limited and more testing is necessary. There is a need to study the

kinetics and equilibrium parameters of iron-oxide coated with different sands for arsenic removal to achieve the permissible concentration in drinking water. However, there is hardly any reported work on the kinetics and equilibrium studies on As(III) removal from contaminated water by IOCQS, iron oxide-coated lignite sand (IOCLS) and iron oxide-coated silica sand (IOCSS). The objectives of this work are to study the feasibility of IOCQS, IOCLS, and IOCSS as adsorbent for arsenic removal from contaminated water. The effects of initial As(III) concentration, the kinetics, and equilibrium isotherm studies for the removal of arsenic from the contaminated water in the presence of IOCQS, IOCLS, and IOCSS have also been undertaken. The kinetics and isotherms parameters obtained in this study can also be compared to provide an economical adsorbent for feasible solution to the arsenic-contaminated drinking water problem with other reported adsorbent systems.

## 2. Models

To understand adsorption phenomena under equilibrium as well as at equilibrium, two types of models are normally developed on the basis of agitation period (kinetics modeling) as well as initial arsenic concentration (equilibrium modeling) as stated below:

### 2.1. Kinetics modeling

Different kinetic models, such as pseudo-first-order model, pseudo-second-order model, Weber and Morris model, Elovich model, etc. are normally used to describe the nonequilibrium stage of adsorption [27]. In brief, the original forms of these models and the linear forms of these models are described as follows:

#### 2.1.1. Pseudo-first-order model

Lagergren [28] showed that the rate of adsorption of pollutants on the adsorbent follows a pseudo-first-order model.

$$\frac{dq_t}{dt} = k_f(q_e - q_t) \quad \text{or} \\ \log(q_e - q_t) = \log q_e - \frac{k_f}{2.303} t \quad (1)$$

where  $q_e$  and  $q_t$  are the sorption capacity (mg/g) of adsorbent at equilibrium and at time  $t$  (min), respectively, and  $k_f$  is the pseudo-first-order sorption rate constant ( $s^{-1}$ ).

### 2.1.2. Pseudo-second-order model

Ho and McKay [29] proposed the pseudo-second-order kinetic model for the sorption process as described below:

$$\frac{dq_t}{dt} = k_s(q_e - q_t)^2 \quad \text{or} \quad \frac{t}{q_t} = \frac{1}{k_s q_e^2} + \frac{1}{q_e} t \quad (2)$$

where  $k_s$  is the pseudo-second-order sorption rate constant (g/mg s); at  $t \rightarrow 0$ ,  $k_s q_e^2$  represents the rate of adsorption and hence, it is termed as initial sorption rate,  $h$  (mg/g s).

### 2.1.3. Weber and Morris model

Weber and Morris [30] described the intraparticle uptake of the sorption process to be proportional to the half-power of time:

$$q_t = k_{id} t^{1/2} + C \quad (3)$$

where  $k_{id}$  is intraparticle diffusion rate constant (mg/g/s<sup>1/2</sup>) and  $C$  (mg/g) is a constant that gives idea about the thickness of the boundary layer, i.e. larger the value of  $C$ , the greater is the boundary-layer effect.

### 2.1.4. Elovich model

Elovich model [31] describes the chemisorption phenomena in which desorption is negligible. In this model, the rate of adsorption decreases due to the increase in the surface coverage of adsorbent with time as in the following statement:

$$\frac{dq_t}{dt} = \alpha \exp(-\beta q_t) \quad (4)$$

where  $\alpha$  is the initial sorption rate constant (mg g<sup>-1</sup> min<sup>-1</sup>) and  $\beta$  is the desorption constant (g/mg). Chien and Clayton [32] simplified the equation assuming  $\alpha\beta t \gg 1$  and applying the boundary conditions,  $t=0$  to  $t=t$ , and  $q_t=0$  to  $q_t=q_t$  as:

$$q_t = \ln(\alpha\beta)/\beta + \ln(t)/\beta \quad (5)$$

## 2.2. Equilibrium modeling

Adsorption isotherm indicates the relationship between equilibrium adsorption capacity and equilibrium concentration. The overall adsorption process can be modeled by monocomponent and multicomponent isotherms. Commonly used monocomponent

isotherm models are Langmuir, Freundlich, and Temkin isotherms and for multicomponent isotherms, Redlich–Peterson (R–P) was used. Various isotherm equations like those of Freundlich, Langmuir, and R–P have been used to describe the equilibrium characteristics of adsorption.

The Freundlich isotherm [33] is derived by assuming a heterogeneous surface with a nonuniform distribution of heat of adsorption over the surface. Whereas, in the Langmuir theory [34], the basic assumption is that the sorption takes place at specific homogeneous sites within the adsorbent.

The R–P isotherm [35] can be described as follows:

$$q_e = \frac{K_R C_e}{1 + a_R C_e^\beta} \quad \text{or} \quad \ln\left(K_R \frac{C_e}{q_e} - 1\right) = \ln a_R + \beta \ln C_e \quad (6)$$

where  $K_R$  is R–P isotherm constant (1/g),  $a_R$  is R–P isotherm constant (1/mg) and  $\beta$  is the exponent which lies between 0 and 1,  $C_e$  is the equilibrium liquid-phase concentration (mg/L).

For high concentrations, Eq. (6) reduces to Freundlich isotherm

$$q_e = K_F C_e^{1/n} \quad \text{or} \quad \ln q_e = \ln K_F + n \ln C_e \quad (7)$$

where  $K_F = K_R/a_R$  is the Freundlich constant (1/mg), and  $(1/n) = (1 - \beta)$  is the heterogeneity factor.

For  $\beta = 1$ , Eq. (6) reduces to Langmuir equation, i.e.

$$q_e = \frac{q_m K_L C_e}{1 + K_L C_e} \quad \text{or} \quad \frac{C_e}{q_e} = \frac{C_e}{q_m} + \frac{1}{K_L q_m} \quad (8)$$

where  $K_L (=a_R)$  is the Langmuir adsorption constant (1/mg) related to the energy of adsorption and  $q_m (=K_R/a_R)$  signifies adsorption capacity (mg/g).

Another equation used in the analysis of isotherms was proposed Temkin isotherm [36]. Temkin isotherm contains a factor that explicitly takes into account, adsorbing species–adsorbate interactions. This isotherm assumes that (i) the heat of adsorption of all the molecules in the layer decreases linearly with coverage due to adsorbate–adsorbate interactions, and (ii) adsorption is characterized by a uniform distribution of binding energies up to some maximum binding energy [36,37]. Temkin isotherm is represented by following equation:

$$q_e = \frac{RT}{b} \ln(K_T C_e) \quad \text{or} \quad q_e = B_1 \ln K_T + B_1 \ln C_e \quad (9)$$

where  $B_1 = \frac{RT}{b}$ ,  $K_T$  is the equilibrium binding constant (1/mol) corresponding to the maximum binding energy and constant  $B_1$  is related to the heat of adsorption.

To find out the kinetic parameters and isotherm constants, the original forms of kinetic and isotherm equations are converted to linear forms as described previously. The slope and intercepts of derived linear forms of the kinetic and isotherm equations are used to determine the isotherm constants. For each system kinetic and isotherm, all the experimental data were used. The kinetic parameters, isotherm constants, and the correlation coefficient,  $R^2$ , are determined by using the solver add-in function of the MS Excel for the fitting of the experimental data.

### 2.3. Error analysis

In this study, nonlinear error functions were examined. In each case, a set of parameters were determined by minimizing the respective error function across the concentration range.

The sum of the squares of the errors (SSE) is given as:

$$\text{SSE} = \sum_{i=1}^n (q_{e,\text{cal}} - q_{e,\text{exp}})_i^2 \quad (10)$$

## 3. Materials and methods

### 3.1. Chemicals

All the chemicals used in the study were of analytical-reagent grade. A solution of As(III) was prepared in double-distilled water by dissolving 0.1734 g of sodium arsenite ( $\text{NaAsO}_2$ ) in 1,000 ml volumetric flask. Standard acid and base solutions (0.5 M  $\text{H}_2\text{SO}_4$  and 1 M NaOH) were used for pH adjustments. In arsenic adsorption process, the pH of the solution increases with time, thus, after every 2 h of agitation, the solution pH was measured and adjusted with 0.5 M  $\text{H}_2\text{SO}_4$ .

### 3.2. Preparation of adsorbents

Three adsorbents IOCQS, IOCLS, and IOCSS were used in this study. These adsorbents were prepared using the procedure adopted in our previous study [1,2]. The quartz, lignite, and silica sand used in this study were obtained from local quarry from the bank of river Yamuna from mining area near Shankargarh, Allahabad (India). In order to remove any fines attached to these particles and leachable matter, this was further washed several times with distilled water. The quartz, lignite, and silica sand were considered fit for use only when the distilled water obtained after washing them was evidently clear. After this, these

were dried in an oven at 103–110°C. The quartz, lignite, and silica sand were then sieved to the geometric mean (GM) sizes of 547.72, 547.72, and 547.72  $\mu\text{m}$  by standard sieves. GM size of particles is equal to  $(d_1 d_2)^{0.5}$ , where  $d_1$  and  $d_2$  are the sieve openings in mm for particles retained and particles passed, respectively. These sands were acid-soaked in 1.0 M HCl solution for 24 h to remove the foreign substance and dust followed by rinsing with distilled water. The sand was oven-dried later at 103°C. Dried sand was stored in PVC cans for further processing to oxide-coated quartz, lignite, and silica sand.

The iron-coated sands were prepared by mixing 50 g ferric nitrate ( $\text{Fe}(\text{NO}_3)_3 \cdot 9\text{H}_2\text{O}$ ) and 150 ml distilled water in iron bowl for 10 min using a glass rod and until all ferric nitrates were dissolved. About 250 g quartz sand was poured in the bowl and the total mixture was again mixed for about 20 min with the glass rod. The total mixture was heated until dry with frequent mixing of sand with solution. The coated sands were cooled at room temperature and washed with tap water until the supernatant was clear. The washed coated sands were then dried in an oven at  $103 \pm 2^\circ\text{C}$ . The coated sands were cooled and stored in plastic jars for further use.

### 3.3. Analytical procedures

The concentrations of As(III) present in the solution were measured by a spectrophotometer (model Genesys-20), Thermo Spectronic (USA). The maximum wavelength for arsenic was determined to be 865 nm. The calibration curves were then prepared by reading absorbance at the maximum wavelength against the known amount of the As(III) present in the solution. The pH values of the aqueous solution of arsenic were monitored by a digital pH meter (model 420A +, Thermo Orion, USA).

### 3.4. Batch experimental programmer and kinetics and equilibrium study

In order to understand the adsorption pattern of the adsorbate on the IOCQS, IOCLS, and IOCSS, the effects of various operating parameters like pH, As(III) initial concentration, and adsorbent dose was performed in 300 ml biological oxygen demand (BOD) bottles with various concentrations of arsenic. For each batch experiment with all three coated sands, one of the following parameters was varied while the others were kept constant: pH, temperature, arsenic concentration, and adsorbent dose. For each experiment, 100 ml of the aqueous solution of known As(III) concentration, pH, and a known amount of the

adsorbents were taken in a 300 ml Stoppard BOD bottles. This mixture was agitated at a temperature of 30 °C in rotary shaker at constant speed of (40 ± 1) rpm. A small amount of the sample was withdrawn with time and was filtered through Whatman filter paper No. 42 (pore size 2.5 μm) and analyzed for arsenic concentration by spectrophotometer.

To study the effect of initial pH (4–11) of all three adsorbents on As(III) uptake, the experiments were performed with initial arsenic concentrations of 500 μg/l and adsorbent dose of 20 g/l at a fixed contact time of 6 h. Isotherm studies were conducted with varying initial As(III) concentrations (300–2,100 μg/l) at fixed adsorbents dose of 20 g/l and varying adsorbents dose (5–35 mg/l) at fixed As(III) concentration 500 μg/l, and contact time of 6 h at pH 7.0. The effect of contact time was studied with an initial As(III) concentration of 500 μg/l and adsorbent dose of 20 g/l; pH was kept at 7.0 and contact time was varied from 0 to 450 min. The effect of adsorbent dose was studied by varying the dose from 5 to 35 g/l at a fixed pH of 7.0 with an initial As(III) concentration of 500 μg/l and contact time of 6 h.

## 4. Results and discussion

### 4.1. Effect of pH

The pH of the solution affects the surface charge of the adsorbents, as well as the degree of ionization and speciation of different pollutants [38]. Change in pH affects the adsorptive process through dissociation of functional groups on the adsorbent surface-active sites. This subsequently leads to a shift in reaction kinetics and equilibrium characteristics of adsorption process. Adsorption of various anionic and cationic species on such adsorbents has been explained on the basis of the competitive adsorption of H<sup>+</sup> and OH<sup>-</sup> ions with the adsorbates [39]. It is a common observation that the surface adsorbs anions favorably at lower pH due to the presence of H<sup>+</sup> ions, whereas, the surface is active for the adsorption of cations at higher pH due to the deposition of OH<sup>-</sup> ions [40].

The effect of variation of the initial solution pH (3–10) on the adsorption of As(III) is illustrated in Fig. 1. The data in Fig. 1 reveal that the removal efficiency of As(III) increases with an increase in pH from 4 to 7 and remains almost constant on further increase in pH up to 9 for IOCQS, IOCLS, and IOCSS adsorbents but the removal efficiency drastically decreases with further increase in pH above 7, in case of IOCLS. The maximum 96% removal of As(III) was observed between pH range 6–7 for all the three adsorbents. The oxides of alumina, calcium, and silica

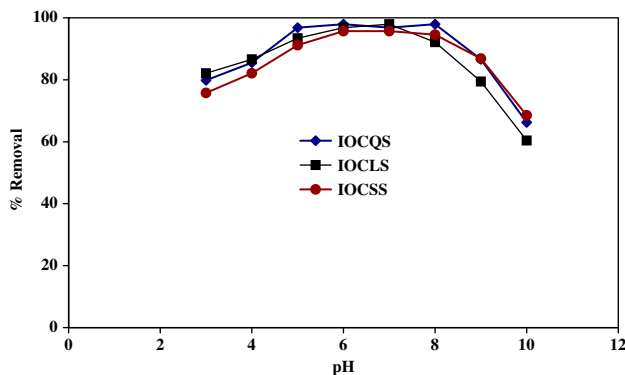


Fig. 1. Effect of pH on the removal of As(III). *T*: 30 °C; *t*: 6 h; *C*<sub>0</sub>: 500 μg/l; IOCQS, IOCLS, and IOCSS dosage: 20 g/l; rpm: (40 ± 1).

present in IOCQS, IOCLS, and IOCSS develop charge on contact with water. Except silica, all other oxides possess positive charge in the pH range of interest because zero-point charges of SiO<sub>2</sub>, Al<sub>2</sub>O<sub>3</sub>, and CaO are 2.2, 8.3, and 11.0, respectively. In the solution, Fe<sup>3+</sup> exists as positively charged species, such as Fe(OH)<sub>2</sub><sup>+</sup> and Fe(OH)<sup>2+</sup> and as neutral species like Fe(OH)<sub>3</sub>. With an increase in the value of pH, the relative amounts of positively charged species decrease and the relative amount of neutral species increase. At pH 5.8 ± 0.2, both Fe(OH)<sub>2</sub><sup>+</sup> and Fe(OH)<sup>2+</sup> coexist. However, the relative amount of Fe(OH)<sup>2+</sup> is more than that of Fe(OH)<sub>2</sub><sup>+</sup>. At pH 8 and 12, the predominating species are Fe(OH)<sub>2</sub><sup>+</sup> and Fe(OH)<sub>3</sub>, respectively [6]. The positively charged hydroxides of iron can be chemisorbed on the negatively charged sites on IOCQS, IOCSS, and IOCLS surfaces created by the oxides present in the sand. We can see from the figure that a similar behavior of As(III) removal was observed for IOCQS and IOCSS, but a different pattern was observed in the case of IOCLS. Similar results have also been reported [18] using iron oxide-coated sand: removal of As(III) and As(IV) was

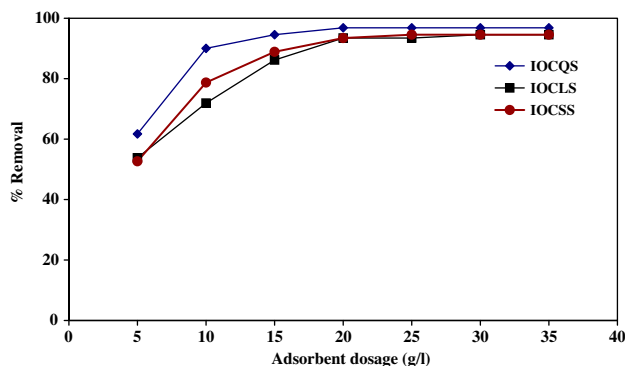


Fig. 2. Effect of adsorbent dose on the removal of As(III). pH: 7.0; *T*: 30 °C; *t*: 6 h; *C*<sub>0</sub>: 500 μg/l; rpm: (40 ± 1).

greater than 95% in the pH range 5–7.6 after 6 h of contact time with an initial arsenic concentration of 100 µg/l. Maximum As(III) uptake was observed at pH 7.5, and hence, all further experiments were carried out at pH of 7.5.

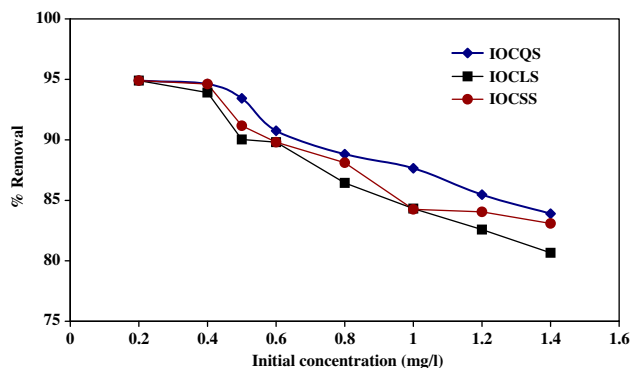


Fig. 3. Effect of initial As(III) concentrations on removal of As(III). pH: 7.0;  $T$ : 30°C;  $t$ : 6 h; IOCQS, IOCLS, and IOCSS dosage: 20 g/l; rpm:  $(40 \pm 1)$ .

#### 4.2. Effect of adsorbent dosage ( $m$ )

The effect of  $m$  on the uptake of As(III) on IOCQS, IOCLS, and IOCSS was studied and is shown in Fig. 2. This figure reveals that the removal of As(III) increases very rapidly with an increase in adsorbent dosage from 5 to 20 g/l and then, it remains almost constant. The removal of As(III) at adsorbent dosage larger than 20 g/l remains almost unchanged. At 20 g/l As(III), a percentage removal of above 95% for all three adsorbents was observed. The increase in the efficiency of removal may be attributed to the fact that with an increase in the adsorbent dose, more adsorbent surface is available for the solute to be adsorbed. Same trend was also observed by Gupta et al. for the adsorption of As(III) from aqueous solutions by iron-oxide-coated sand [18]. At  $m < 20$  g/l, the adsorbent surface becomes saturated with As(III) and the residual concentration in the solution is large. With increase in  $m$ , the As(III) removal increases due to increased As(III) uptake by the increased amount of adsorbent. At  $m > 20$  g/l, the increment in As(III) removal becomes very low as the surface As(III) concentration and the solution As(III) concentration come to equilibrium with each other. It can be seen that the As(III) removal becomes almost constant at

Table 1  
Kinetic parameters of various kinetic models for removal of As(III) by three adsorbents (IOCQS, IOCLS, and IOCSS)

Model	$q_{e,exp}$	$q_{e,cal}$	Kinetics parameters	$R^2$	Error, SSE
<b>IOCQS</b>					
Pseudo-first-order	0.02449	0.00585	$k_f$ ( $\text{min}^{-1}$ ): 0.0062	0.9628	$2.47 \times 10^{-3}$
Pseudo-second-order	0.02449	0.02522	$k_s$ ( $\text{min}^{-1}$ ): 2.3111	0.9982	$2.15 \times 10^{-5}$
Weber and Morris model	–	–	$k_{id}$ ( $\text{mg g}^{-1} \text{min}^{-1/2}$ ): 0.00028 $C$ ( $\text{mg g}^{-1}$ ): 0.0187	0.9887	$3.635 \times 10^{-7}$
Elovich model	–	–	$\alpha$ ( $\text{mg g}^{-1} \text{min}^{-1/2}$ ): 13.2941 $\beta$ ( $\text{g mg}^{-1}$ ): 625	0.9496	$1.591 \times 10^{-6}$
<b>IOCLS</b>					
Pseudo-first-order	0.0244	0.00455	$k_f$ ( $\text{min}^{-1}$ ): 0.00299	0.9524	$2.85 \times 10^{-3}$
Pseudo-second-order	0.0244	0.09621	$k_s$ ( $\text{min}^{-1}$ ): 2.0616	0.9912	$3.02 \times 10^{-5}$
Weber and Morris model	–	–	$k_{id}$ ( $\text{mg g}^{-1} \text{min}^{-1/2}$ ): 0.00027 $C$ ( $\text{mg g}^{-1}$ ): 0.0184	0.9568	$1.35 \times 10^{-6}$
Elovich model	–	–	$\alpha$ ( $\text{mg g}^{-1} \text{min}^{-1/2}$ ): 23.67 $\beta$ ( $\text{g mg}^{-1}$ ): 666.67	0.9038	$2.982 \times 10^{-6}$
<b>IOCSS</b>					
Pseudo-first-order	0.0242	0.00853	$k_f$ ( $\text{min}^{-1}$ ): 0.00875	0.8803	$1.74 \times 10^{-3}$
Pseudo-second-order	0.0242	0.02521	$k_s$ ( $\text{min}^{-1}$ ): 1.8752	0.9942	$2.91 \times 10^{-5}$
Weber and Morris model	–	–	$k_{id}$ ( $\text{mg g}^{-1} \text{min}^{-1/2}$ ): 0.00033 $C$ ( $\text{mg g}^{-1}$ ): 0.0174	0.96005	$1.92 \times 10^{-6}$
Elovich model	–	–	$\alpha$ ( $\text{mg g}^{-1} \text{min}^{-1/2}$ ): 2.4649 $\beta$ ( $\text{g mg}^{-1}$ ): 555.56	0.90315	$4.549 \times 10^{-6}$

Note: –, not applicable.

$m = 20$  g/l. Optimum IOCQS, IOCLS, and IOCSS doses were found to be 20 g of each adsorbent per litre of As(III) solution. Here, optimum adsorbent dose of all three adsorbents are approximately the same. This may be one reason for very little difference between the As(III) uptake by all the three adsorbents.

#### 4.3. Effect of initial arsenic concentration ( $C_0$ )

The effect of  $C_0$  on the removal of As(III) by the adsorbents at optimum dosage of each adsorbent is shown in Fig. 3. From the figure, it is evident that the As(III) removal decreased with the increase in  $C_0$ , although the actual amount of As(III) adsorbed per unit mass of adsorbent increased with the increase in  $C_0$ . Fig. 3 reveals that removal efficiency is higher (96%) with a lower initial As(III) concentration (0.2 mg/l); a gradual decrease in As(III) uptake was observed at higher initial concentrations of As(III). The pattern of all the three adsorbents is the same. The maximum removal efficiencies at higher As(III) concentration of 1.4 mg/l are 85, 83.5, and 81% for IOCQS, IOCLS, and IOCSS sand, respectively. The reason for the decrease in As(III) adsorption efficiency at higher initial concentrations may be that the adsorbent sites eventually become saturated with adsorbed arsenic and at this point, further addition of arsenic to the solution would not be expected to increase the amount adsorbed significantly [18].

#### 4.4. Adsorption kinetic study

Normally, four types of kinetic models, such as pseudo-first-order, pseudo-second-order, Weber and Morris, and Elovich model, etc. are used to describe the nonequilibrium stage of adsorption. The details of general equation and linear form of these models are described in Section 2.1. To estimate the kinetic parameters associated with different kinetic models are reported in Table 1 and specific uptake of As(III) on IOCQS, IOCLS, and IOCSS with agitation time is plotted in Fig 4.

The values of adsorption rate constant ( $k_f$ ) for As(III) adsorption on IOCQS, IOCLS, and IOCSS were determined from the plot of  $\log(q_e - q_t)$  against  $t$  (not shown). These  $k_f$  values ( $k_f = 4.33 \times 10^{-6} \text{ min}^{-1}$  for IOCQS,  $0.00299 \text{ min}^{-1}$  for IOCLS, and  $0.00691 \text{ min}^{-1}$  for IOCSS) (Table 1) and  $q_{e,exp}$  and  $q_{e,cal}$  of the three adsorbents are very different. This shows that the pseudo-first-order is not fitted well for As(III) removal. In the present work,  $k_f$  values of all adsorbents are within range of reported values of  $4.22 \times 10^{-5} \text{ min}^{-1}$  for the adsorption of As(III) on GAC-Fe [6].

Fig. 4(a) shows the plot of  $t/q_t$  vs.  $t$ . The equilibrium adsorption capacity,  $q_e$  is obtained from the slope of the plot. Since  $q_e$  is known from the slope, the pseudo-second-order constant  $k_s$  can be calculated from Fig. 4(a) and listed in Table 2. The  $q_{e,exp}$  and the  $q_{e,calc}$  values along with calculated correlation coefficients for the pseudo-first-order model and pseudo-second-order models are shown in Table 2. The  $q_{e,exp}$

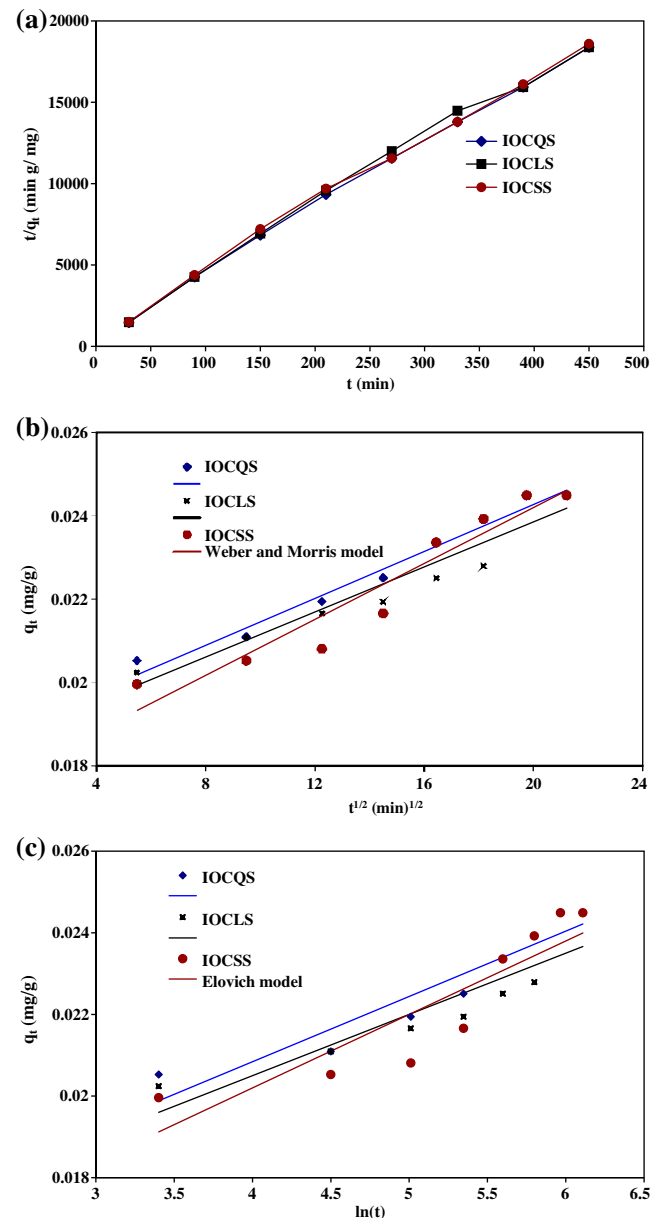


Fig. 4. Kinetic analysis by (a) Pseudo-second-order kinetic (b) Weber and Morris intraparticle diffusion (c) Elovich model plots for the removal of As(III) by various adsorbents (pH: 7.0; T: 30°C;  $C_0$ : 500  $\mu\text{g/l}$ ; IOCQS, IOCLS, and IOCSS dosage: 20 g/l; rpm:  $(40 \pm 1)$ ).

and the  $q_{e,calc}$  values from the pseudo-second-order kinetic model are very close to each other. The calculated correlation coefficients are also closer to each other for pseudo-second-order kinetics than that for the pseudo-first-order kinetic model. Therefore, the sorption can be approximated more appropriately by the pseudo-second-order kinetic model than the pseudo-first-order kinetic model for all the three adsorbents. Mondal et al. [6] reported a  $k_s$  value of 0.0602 and 0.1383 g/mg/s for the adsorption of As(III) and As(V) on GAC-Fe, respectively. Due to difference in the nature of the adsorbents used in this work, a direct comparison of the values of  $k_s$  is not possible with the reported values.

Fig. 4(b) presents a plot of  $q_t$  vs.  $t^{1/2}$  for all the three adsorbents. The value of  $C$  (Table 1) gives an

idea about the thickness of the boundary layer, i.e. the larger the intercept, the greater is the boundary-layer effect [41]. The values of  $k_{id}$  and  $C$  as obtained from the plots are listed in Table 2. The deviation of the straight lines from the origin may be due to the difference in the rate of mass transfer during the initial and final stages of adsorption. The figure reveals that the plots  $q_t$  vs.  $t^{1/2}$  exhibit the linearity of all the three adsorbents, which indicates that only pore diffusion controls the adsorption model for As(III) removal. The slope of the Weber and Morris plots  $q_t$  vs.  $t^{1/2}$  are defined as a rate parameter characteristic of the rate of adsorption in the region where intraparticle diffusion is rate-controlling. The more straight line portion is attributed to diffusion due to intraparticle macropore diffusion. This figure also reveals that

Table 2  
Isotherm parameters and error analysis for removal of As(III) by three adsorbents (IOCQS, IOCLS, and IOCSS)

Model	At different doses			At different As(III) concentration		
	Kinetics parameters	$R^2$	Error, SSE	Kinetics parameters	$R^2$	Error, SSE
<i>IOCQS</i>						
Langmuir	$q_m$ (mg g <sup>-1</sup> ): 0.1348 $K_L$ (1 mg <sup>-1</sup> ): 12.685	0.9633	$4.89 \times 10^{-4}$	$q_m$ (mg g <sup>-1</sup> ): 0.2283 $K_L$ (1 mg <sup>-1</sup> ): 1.7837	0.9821	$1.75 \times 10^{-4}$
Freundlich	$K_f$ (1 mg <sup>-1</sup> ): 0.65004 $n$ : 1.2084	0.9815	$2.09 \times 10^{-4}$	$K_f$ (1 mg <sup>-1</sup> ): 0.1803 $n$ : 1.4698	0.9825	$2.58 \times 10^{-4}$
R–P	$K_R$ (1 g <sup>-1</sup> ): 455.05 $a_R$ (1 mg <sup>-1</sup> ): 981.016 $\beta_1$ : 0.2951	0.9757	$4.12 \times 10^{-4}$	$K_R$ (1 g <sup>-1</sup> ): 1.4559 $a_R$ (1 mg <sup>-1</sup> ): 6.9729 $\beta_1$ : 0.349552	0.9834	$1.97 \times 10^{-4}$
Temkin	$B_1$ (mg g <sup>-1</sup> ): 0.0357 $K_T$ (1 mg <sup>-1</sup> ): 100.77	0.9494	$3.64 \times 10^{-4}$	$B_1$ (mg g <sup>-1</sup> ): 0.0298 $K_T$ (1 mg <sup>-1</sup> ): 39.0877	0.9162	$7.15 \times 10^{-4}$
<i>IOCLS</i>						
Langmuir	$q_m$ (mg g <sup>-1</sup> ): 0.0449 $K_L$ (1 mg <sup>-1</sup> ): 10.8361	0.9441	$4.49 \times 10^{-5}$	$q_m$ (mg g <sup>-1</sup> ): 0.2102 $K_L$ (1 mg <sup>-1</sup> ): 9.1247	0.9841	$1.89 \times 10^{-4}$
Freundlich	$K_f$ (1 mg <sup>-1</sup> ): 0.05871 $n$ : 2.3568	0.9439	$4.51 \times 10^{-5}$	$K_f$ (1 mg <sup>-1</sup> ): 0.492499 $n$ : 1.467	0.9845	$1.74 \times 10^{-4}$
R–P	$K_R$ (1 g <sup>-1</sup> ): 1.3161 $a_R$ (1 mg <sup>-1</sup> ): 23.357 $\beta_1$ : 0.680171	0.9456	$4.38 \times 10^{-5}$	$K_R$ (1 g <sup>-1</sup> ): 19.8541 $a_R$ (1 mg <sup>-1</sup> ): 40.4437 $\beta_1$ : 0.3422	0.9846	$1.74 \times 10^{-4}$
Temkin	$B_1$ (mg g <sup>-1</sup> ): 0.0104 $K_T$ (1 mg <sup>-1</sup> ): 92.3005	0.9464	$4.31 \times 10^{-5}$	$B_1$ (mg g <sup>-1</sup> ): 0.0325 $K_T$ (1 mg <sup>-1</sup> ): 169.7125	0.9601	$4.45 \times 10^{-4}$
<i>IOCSS</i>						
Langmuir	$q_m$ (mg g <sup>-1</sup> ): 0.1225 $K_L$ (1 mg <sup>-1</sup> ): 5.5396	0.9789	$8.07 \times 10^{-5}$	$q_m$ (mg g <sup>-1</sup> ): 0.2212 $K_L$ (1 mg <sup>-1</sup> ): 2.7945	0.981	$2.03 \times 10^{-4}$
Freundlich	$K_f$ (1 mg <sup>-1</sup> ): 0.2019 $n$ : 1.4585	0.9849	$5.62 \times 10^{-5}$	$K_f$ (1 mg <sup>-1</sup> ): 0.246 $n$ : 1.4468	0.9861	$1.99 \times 10^{-4}$
R–P	$K_R$ (1 g <sup>-1</sup> ): 185.0036 $a_R$ (1 mg <sup>-1</sup> ): 915.54 $\beta_1$ : 0.3151	0.9849	$5.62 \times 10^{-5}$	$K_R$ (1 g <sup>-1</sup> ): 14.3689 $a_R$ (1 mg <sup>-1</sup> ): 59.834 $\beta_1$ : 0.3459	0.9849	$2.43 \times 10^{-4}$
Temkin isotherm	$B_1$ (mg g <sup>-1</sup> ): 0.0224 $K_T$ (1 mg <sup>-1</sup> ): 74.7499	0.9692	$1.14 \times 10^{-4}$	$B_1$ (mg g <sup>-1</sup> ): 0.0325 $K_T$ (1 mg <sup>-1</sup> ): 58.2748	0.9412	$6.07 \times 10^{-4}$

micropore diffusion is not applicable, it may be one of the reasons that the size of the micropores of all the three adsorbents is less than the average size of As(III) (48 nm) [6]. The values of rate parameters ( $k_{id}$  and  $C$ ) of the three adsorbents as given in Table 1 show that  $k_{id}$  values of all adsorbents are same but there are minute differences in their  $C$  values. Mondal et al. [6] reported  $k_{id}$  values,  $7.74 \times 10^{-4}$ ,  $3.87 \times 10^{-4}$ , and  $7.74 \times 10^{-4}$  and  $C$  values, 0.031, 0.017, and 0.31 for As(III), As(V), and As(T), respectively. These values are very similar to the values reported in Table 1 in this study. They show that the Weber-Morris model shows better representation of the data than the pseudo-first-order kinetic model.

The Elovich model, an empirical chemisorption model, was originally developed to describe the kinetics of heterogeneous chemisorption of gases on a solid surface. The Elovich model has been used to describe the kinetics of sorption and desorption of various inorganic materials on many sorbents [42,43]. Elovich plot of  $q_t$  vs.  $\ln(t)$  for all the three adsorbents could indicate a changeover from one type of binding site to another type of site having different reaction kinetics [32,44]. In this work, a two-stage Elovich plot can be observed. The first relatively steeper stage of all adsorbents indicates a fast adsorption reaction that takes place on the outer layer and readily available sites, and the second almost small horizontal stage could involve the inner layer of not-readily available sites, such as adsorption sites located in the micropores. The value of  $\beta$  as compared with  $\alpha$  is very high. Therefore, as per Elovich equation, the slope of curve is less and observed wider range for the first stage. The wider range of the first stage is attributed to the diffusion due to intraparticle macropore diffusion and this statement is also supported by Weber and Morris model for intraparticle diffusion model. Fig. 4(c) summarizes the experimental data along with model predictions using the Elovich model. The agreement between the experimental data-set and the model-fitting curves is indicated by high coefficients of determination for the Weber and Morris model (illustrated in Fig. 4(b) and (c)). It indicates that the Weber and Morris model has good model applicability for the experimental data, which can be utilized to explain the overall kinetics of As(III) adsorption on all the three adsorbents.

#### 4.5. Adsorption equilibrium study

To optimize the design of an adsorption system for the removal of adsorption of adsorbates, it is important to establish the most appropriate correlation for the equilibrium curves. Various isotherm equations

have been used to describe the equilibrium nature of adsorption. Most of researchers have used Freundlich [33] and Langmuir isotherms [35] to represent equilibrium adsorption data using iron-coated sands-arsenic contaminants systems [3,18]. But these equations have serious limitations on their usage, the most popular Freundlich isotherm is suitable for highly heterogeneous surfaces, however, it is valid for adsorption data over a restricted range of concentrations. For highly heterogeneous surfaces and extremely low concentrations, Henry's law is valid. However, Freundlich equation does not approach Henry's law at vanishing concentrations. The Langmuir equation although follows Henry's law at vanishing concentrations, is valid for homogeneous surfaces. Thus, both these isotherm equations may not be suitable for As(III) adsorption on activated carbons and for the whole range of concentrations used in the study. Temkin isotherm contains a factor that explicitly takes into account the interactions between adsorbing species and the adsorbate. This isotherm assumes that (i) the heat of adsorption of all the molecules in the layer decreases linearly with coverage due to adsorbate-adsorbate interactions, and (ii) adsorption is characterized by a uniform distribution of binding energies, up to some maximum binding energy [36,37]. The R-P equation [35], a three-parameter equation, is often used to represent solute adsorption data on heterogeneous surfaces. These equations get reduced to Henry's equation at very low concentrations. Due to experimental limitations, we could not obtain adsorption equilibrium data at very low concentrations. In this study, we tried to use the four isotherm equations given by Langmuir, Freundlich, R-P, and Temkin to fit the experimental data for As(III) on adsorbents IOCQS, IOCLS, and IOCSS. However, to find out the isotherm constants of Langmuir, Freundlich, R-P, and Temkin isotherms, the original forms of these isotherms are converted to linear forms as described in Section 2.2. The slope and intercepts of these derived linear forms of the isotherms are used to determine the isotherm constants.

To determine the equilibrium parameters for the adsorption of As(III) on three-adsorbent surface at different doses, experimental data were used to fit different adsorption isotherms as reported in the Figs. 5 and 6 at different dosages and at different As(III) concentrations, respectively. Parameters calculated for different isotherms for all As(III)-adsorbent systems are tabulated in Table 2 for different dosages and at different As(III) concentrations, respectively. The reported values in this study are very comparable with the reported values in other studies [18]. By comparing the results of the values for the error

function and correlation coefficients (Table 2), similar “best-fit” results for As(III) adsorption on IOCQS, IOCLS, and IOCSS are obtained. Figs. 5 and 6 show the comparative fit of different isotherms with the equilibrium data plotted as  $q_e$  vs.  $C_e$  of the three adsorbents at different initial As(III) concentrations and at different dosage of adsorbents, respectively. It is clear from Figs. 5 and 6 that among the conventional isotherms, the Freundlich isotherm provides

the best prediction of specific uptake followed by R–P, Langmuir, and Temkin for As(III) investigated. Due to the aforementioned fact, Freundlich isotherm provides better prediction for the specific uptake of As(III) for all the three adsorbents. Recently, Freundlich isotherm has also been found to be more suitable to explain the adsorption equilibrium for the adsorption of arsenic species on GAC-Fe [6] and IOCS [18].

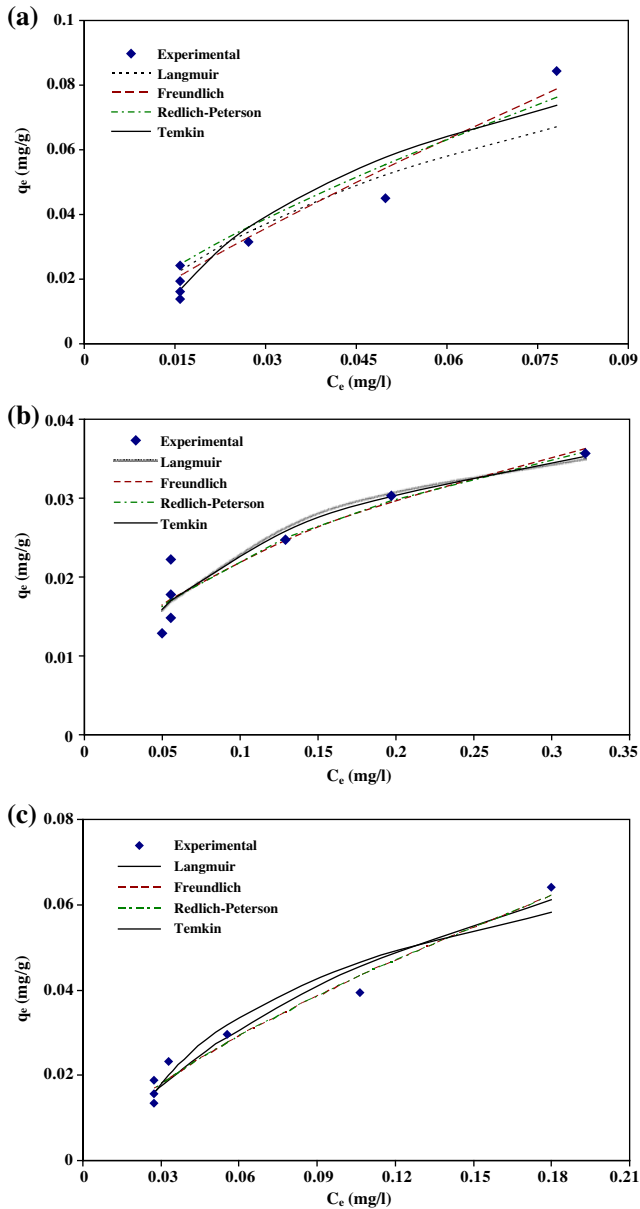


Fig. 5. Langmuir Freundlich, R–P and Temkin isotherm analysis on (a) IOCQS (b) IOCLS (c) IOCSS at different dose for the removal of As(III) (pH: 7.0;  $T$ : 30 °C;  $C_0$ : 500  $\mu\text{g/l}$ ; IOCQS, IOCLS, and IOCSS dosage: 5–35 g/l; rpm:  $(40 \pm 1)$ ).

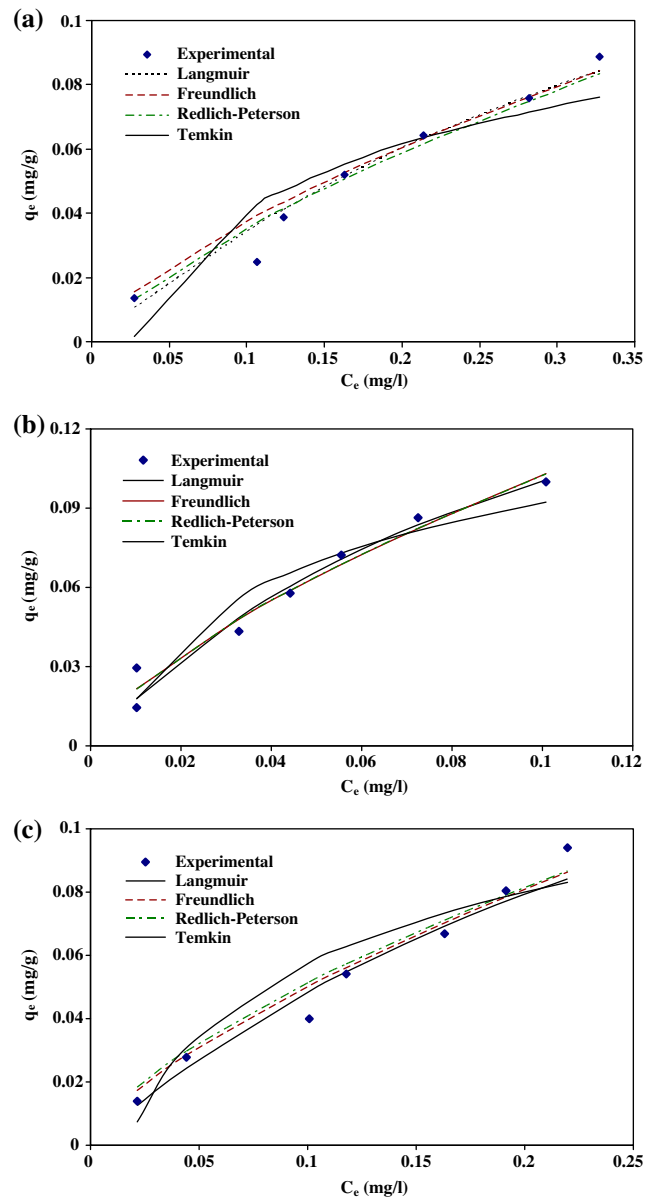


Fig. 6. Langmuir Freundlich, R–P and Temkin isotherm analysis on (a) IOCQS (b) IOCLS (c) IOCSS at different initial As(III) concentration for the removal of As(III) (pH: 7.0;  $T$ : 30 °C;  $C_0$ : 300–2,100  $\mu\text{g/l}$ ; IOCQS, IOCLS, and IOCSS dosage: 20 g/l; rpm:  $(40 \pm 1)$ ).

#### 4.6. Determination of diffusivity

Kinetic data could be treated by models given by Boyd et al. [45] which is valid under the experimental conditions used. With diffusion rate controlling in the adsorption particles of spherical shape, the diffusion coefficients for As(III) of all the three adsorbents have been computed from Vermeulen's approximation [46] which fits the whole range,  $0 < F(t) < 1$ , for adsorption on spherical particles.

$$F(t) = \left[ 1 - \exp\left(\frac{-\pi^2 D_e t}{R_a^2}\right) \right]^{1/2} \quad (11)$$

This equation could further be simplified to cover most of the data points for calculating effective particle diffusivity.

$$\ln\left[\frac{1}{(1 - F^2(t))}\right] = \frac{\pi^2 D_e t}{R_a^2} \quad (12)$$

where  $F(t) = q_t/q_e$  is the fractional attainment of equilibrium at time  $t$ ,  $D_e$  is the effective diffusion coefficient of adsorbates in the adsorbent phase ( $\text{m}^2/\text{s}$ ),  $R_a$  is radius of the adsorbent particle assumed to be spherical (m). Thus, the slope of the plot of  $\ln[1/(1 - F^2(t))]$  vs.  $t$  would give  $D_e$ . The value of  $D_e$  is  $7.725 \times 10^{-9}$ ,  $1.241 \times 10^{-9}$ , and  $8.366 \times 10^{-9} \text{ cm}^2/\text{s}$ , respectively for As(III) adsorption on IOCQS, IOCLS, and IOCSS. According to Michelson et al. [47], if film diffusion is the rate-limiting step, the value of  $D_e$  should be between  $10^{-6}$  and  $10^{-8} \text{ cm}^2/\text{s}$ , but on the other hand, if the pore diffusion is in the rate-limiting step, the  $D_e$  value should be above  $10^{-9} \text{ cm}^2/\text{s}$  for heavy metals [47]. In this study, for As(III), the  $D_e$  values of all three adsorbent is above than  $10^{-9} \text{ cm}^2/\text{s}$ . Therefore, it seems that in this case, pore diffusion is the rate-limiting step for As(III) for all the three adsorbents. This fact is also supported by Weber and Morris for interparticle diffusion model (Fig. 4c). The  $D_e$  value for IOCQS, IOCLS, and IOCSS is very close to each other. It may be possible for one reason that As(III) is absorbed in the outer surface in the same way. But minute difference in  $D_e$  values of all the three adsorbents indicates that adsorption in interior pores may be different.

#### 5. Conclusions

The present study shows that iron-oxide-coated quartz (IOCQS), IOCLS, and IOCSS are effective adsorbents for the removal of As(III) from aqueous solution. Optimum conditions for As(III) removal

were found to be pH 7 and adsorbent dose, 20 g/l of solution. Results shows that As(III) removal was achieved above 95% for the three adsorbents. These adsorbents can be employed for reducing As(III) concentrations to less than  $25 \mu\text{g/l}$  (with 20 g/l adsorbent dose and initial As(III) concentration of  $400 \mu\text{g/l}$ ) in drinking water. This result is below the levels prescribed by Indian Standards for drinking water purposes. Adsorption kinetics was found to follow second-order-kinetic model for As(III), which is more accurate for all the adsorbents investigated when compared with other models, such as pseudo-first-order model, Weber and Morris model, and Elovich model. In this study, the effective diffusion coefficient ( $D_e$ ) value of As(III) is more than the order of  $10^{-9} \text{ cm}^2/\text{s}$ . This order is in-line with that found in the literature for pore diffusion is the rate-limiting step for all adsorbents. Among the conventional models-Langmuir, Freundlich, R-P, and Temkin isotherm models, R-P and Freundlich isotherm models provide better prediction for equilibrium specific uptake for As(III) throughout the whole range of As(III) investigated. Over all, conclusions can be drawn on the basis of previous and present studies that iron-oxide coated on the selected sand has many advantages for the removal of arsenic from aqueous solution.

#### Nomenclature

$1/n$	— heterogeneity factor, dimensionless
$a_R$	— constant of Redlich–Peterson isotherm (l/mg)
$B_1$	— related to the heat of adsorption (mg/g)
$C$	— constant that gives idea about the thickness of boundary layer (mg/g)
$C_e$	— equilibrium concentration liquid phase concentration (mg/l)
IOCQS	— iron-oxide-coated quartz sand
IOCLS	— iron-oxide-coated lignite sand
IOCSS	— iron-oxide-coated silica sand
$k_f$	— rate constant of pseudo- first-order adsorption model ( $\text{min}^{-1}$ )
$k_s$	— rate constant of pseudo- second-order adsorption model (g/mg/s)
$k_{id}$	— interparticles diffusion rate of constant ( $\text{mg/g}/\text{min}^{1/2}$ )
$K_F$	— constant of Freundlich isotherm ( $(\text{mg/g})/(\text{l/mg})^{1/n}$ )
$K_L$	— constant of Langmuir isotherm (l/g)
$K_T$	— equilibrium binding constant corresponding to maximum binding energy (l/g)
$k_R$	— constant of Redlich–Peterson isotherm (l/g)
$q_e$	— equilibrium solid phase concentration (mg/g)
$q_{e, \text{cal}}$	— calculated value of solid phase concentration of adsorbate at equilibrium (mg/g)

$q_{e, \text{exp}}$	— experimental value of solid phase concentration of adsorbate at equilibrium (mg/g)
$q_m$	— maximum adsorption capacity of adsorbent (mg/g)
$q_t$	— amount of adsorbate adsorbed by adsorbent at time $t$ (mg/g)
$R$	— universal gas constant (8.314 J/K mol)
SSE	— sum of square error function
$t$	— time (min)
$T$	— absolute temperature (K)

#### Greek symbol

$\alpha$	— initial adsorption rate constant (mg/g/s)
$\beta$	— desorption constant (g/mg)
$\beta_1$	— constant of Redlich–Peterson isotherm ( $0 < \beta_1 < 1$ )

#### Acknowledgments

The authors express their gratitude to the reviewers for their useful comments. Authors are very thankful for financial support provided by Council of Science and Technology (CST), Lucknow (U.P.), Government of India.

#### References

- [1] R.C. Vaishya, S.K. Gupta, Arsenic removal from groundwater by iron impregnated sand, *J. Environ. Eng. Div. (ASCE)* 129 (2003) 89–99.
- [2] R.C. Vaishya, S.K. Gupta, Coated sand filtration: An emerging technology for water treatment, *J. Water Supply: Res. Technol. (AQUA)* 52(4) (2003b) 299–306.
- [3] R.C. Vaishya, S.K. Gupta, Modeling arsenic (V) removal from water by sulfate-modified iron oxide coated sand (SMIOCS), *Sep. Sci. Technol.* 39(3) (2004) 641–666.
- [4] R.C. Vaishya, S.K. Gupta, Batch kinetic modeling of arsenic removal from water by mixed oxide coated sand (MOCS), *J. Environ. Sci. Eng.* 46(2) (2004) 123–136.
- [5] D. Mohan, C.U. Pittman, Arsenic removal from water/wastewater using adsorbents-A critical review, *J. Hazard. Mater.* 142 (2007) 1–53.
- [6] P. Mondal, B. Mohanty, C.B. Majumder, N. Bhandari, Removal of arsenic from simulated groundwater by GAC-Fe: A modeling approach, *AIChE J.* 55(7) (2009) 1860–1871.
- [7] D.M. Ramakrishna, T. Viraraghavan, Y.C. Jin, Iron oxide coated sand for arsenic removal: Investigation of coating parameters using factorial design approach, *Pract. Periodical Hazard, Toxic, Radioact. Waste Manag. ASCE* 10(4) (2006) 198–206.
- [8] P.L. Smedley, M. Zhan, G. Zhang, Z. Luo, Mobilisation of arsenic and other trace elements in fluvio-lacustrine aquifers of the Huhhot Basin, Inner Mongolia, *Appl. Geochem.* 18(9) (2003) 1453–1477.
- [9] USEPA, Comprehensive Environmental Response, Compensation and Liability Act (CERCLA), 2007.
- [10] P. Mondal, C.B. Majumder, B. Mohanty, Laboratory based approaches for arsenic remediation from contaminated water: recent developments, *J. Hazard. Mater. B* 137 (2006) 464–479.
- [11] P. Mondal, C.B. Majumder, B. Mohanty, Quantitative separation of As(III) and As(V) from a synthetic water solution using ion exchange columns in the presence of Fe and Mn ions, *Clean: Soil, Air, Water* 35(3) (2007) 255–260.
- [12] USEPA Office of Ground water and drinking water, Implementation guidance for the arsenic rule. EPA report-816-D-02-005, Cincinnati, USA, 1998.
- [13] D.K. Nordstrom, Worldwide occurrence of arsenic in ground water, *Science* 296 (2002) 2143–2145.
- [14] P. Mondal, C.B. Majumder, B. Mohanty, Treatment of arsenic contaminated water in a batch reactor by using *Ralstonia eutropha* MTCC 2487 and granular activated carbon, *J. Hazard. Mater.* 153 (2008) 588–599.
- [15] M. Mergeay, S. Monchy, T. Vallaey, V. Auquier, *Ralstonia metallidurans*, a bacterium specifically adapted to toxic metals: Towards a catalogue of metal-responsive genes, *FEMS Microbiol. Rev.* 27 (2003) 385–410.
- [16] K. Suresh, S.R. Prabakaran, S. Sengupta, S. Shivaji, *Bacillus indicus* sp.nov., an arsenic-resistant bacterium isolated from an aquifer in West Bengal, India, *Int. J. Syst. Evol. Microbiol.* 54 (2004) 1369–1375.
- [17] S. Hossain, M.N. Anantharaman, Studies on bacterial growth and arsenic(III) biosorption using *Bacillus subtilis*, *Chem. Biochem. Eng. Q* 20(2) (2006) 209–216.
- [18] V.K. Gupta, V.K. Saini, N. Jain, Adsorption of As(III) from aqueous solutions by iron oxide-coated sand, *J. Colloid Interface Sci.* 288 (2005) 55–60.
- [19] O.S. Thirunavukkarasu, T. Viraraghavan, K.S. Subramanian, Arsenic removal from drinking water using iron oxide-coated sand, *Water Air Soil Pollut.* 142 (2003) 95–111.
- [20] Yoon-Young Chang, Ki-Hoon Song, Jae-Kyu Yang, Removal of As(III) in a column reactor packed with iron-coated sand and manganese-coated sand, *J. Hazard. Mater.* 150(3) (2008) 565–572.
- [21] P. Mondal, C.B. Majumder, B. Mohanty, Effects of adsorbent dose, its particle size and initial arsenic concentration on the removal of arsenic, iron and manganese from simulated ground water by Fe<sup>3+</sup> impregnated activated carbon, *J. Hazard. Mater.* 150 (2008) 695–702.
- [22] W. Chen, R. Parette, J. Zou, F.S. Cannon, B.A. Dempsey, Arsenic removal by iron-modified activated carbon, *Water Res.* 41 (2007) 1851–1858.
- [23] R. Goel, S.K. Kapoor, K. Misra, R.K. Sarma, Removal of arsenic from water by different adsorbents, *Indian J. Chem. Technol.* 11 (2004) 518–525.
- [24] Z. Gu, B. Deng, J. Fang, Preparation and evaluation of GAC-based iron-containing adsorbents for arsenic removal, *Environ. Sci. Technol.* 39 (2005) 3833–3843.
- [25] C.P. Huang, L.M. Vane, Enhancing As(V) Removal by a Fe<sup>2+</sup> treated activated carbon, *J. Water Pollut. Control. Fed.* 61 (1989) 1596–1603.
- [26] J. Moller, A. Ledin, P.S. Mikkelsen, First world wide workshop for junior environmental scientists, Removal of dissolved heavy metals from pre-settled storm water runoff by ironoxide coated sand (IOCS), 2002, pp. 17–25.
- [27] R. Hana, W. Zou, Z. Zhang, J. Shi, J. Yang, Removal of copper (II) and lead (II) from aqueous solution by manganese oxide coated sand I. Characterization and kinetic study, *J. Hazard. Mater. B* 137 (2006) 1384–1395.
- [28] S. Lagergren, About the theory of so called adsorption of soluble substances, *Ksver Vetterskapskad Handl* (1898), 24, 16.
- [29] Y.S. Ho, G. McKay, Pseudo-second-order model for sorption processes, *Process Biochem.* 34 (1999) 451–465.
- [30] W.J. Weber, J.C. Morris, Kinetics of adsorption on carbon from solution, *J. Sanitary Eng. Div, ASCE* 89 (SA2) (1963) 31–59.
- [31] R.S. Juang, M.L. Chen, Application of the Elovich equation to the kinetics of metal sorption with solvent impregnated resins, *Ind. Eng. Chem. Res.* 36 (1997) 813–820.

- [32] S.H. Chien, W.R. Clayton, Application of Elovich equation to the kinetics of phosphate release and sorption in soils, *Soil Sci. Soc. Am. J.* 44(2) (1980) 265–268.
- [33] H.M.F. Freundlich, Constitution and fundamental properties of solids and liquids I, *Solids J. Phys. Chem.* A57 (1906) 385–470.
- [34] I. Langmuir, The adsorption of gases on plane surfaces of glass, mica and platinum, *J. Am. Chem. Soc.* 40(9) (1918) 1361–1404.
- [35] O. Redlich, D.L. Peterson, A useful adsorption isotherm, *J. Phys. Chem.* 63 (1959) 1024–1026.
- [36] M. Temkin, J. Pyzhev, Kinetics of ammonia synthesis on promoted iron catalysts, *Acta Physicochim. URSS* 12 (1940) 327–356.
- [37] Y. Kim, C. Kim, I. Choi, S. Rengraj, J. Yi, Removal using mesoporous alumina prepared via a templating method, *Environ. Sci. Technol.* 38 (2004) 924–931.
- [38] Y.S. Ho, G. McKay, The kinetics of sorption of divalent metal ions onto sphagnum moss peat, *Water Res.* 34(3) (2000) 735–742.
- [39] C. Aharoni, S. Sideman, E. Hoffer, Adsorption of phosphate ions by collodion-coated alumina, *J. Chem. Tech. Biotechnol.* 29 (1979) 404–412.
- [40] E. Tutem, R. Apak, C.F. Unal, Adsorptive removal of chlorophenols from water by bituminous shale, *Water Res.* 32 (1998) 2315–2324.
- [41] K. Kannan, M.M. Sundaram, Kinetics and mechanism of removal of methylene blue by adsorption on various carbons — a comparative study, *Dyes Pigments* 51 (2001) 25–40.
- [42] D.L. Sparks, *Environmental soil chemistry*, Academic, San Diego, CA, 1995.
- [43] D.L. Sparks, *Kinetics and Mechanisms of Chemical Reaction at the Soil Mineral/water Interface. Soil Physical Chemistry*, second ed., CRC, Boca Raton, FL, 1999.
- [44] R. Atkinson, F. Hingston, A. Posner, J. Quirk, Elovich equation for the kinetics of isotope exchange reactions at solid-liquid interface, *Nature (London)* 226 (1970) 148–149.
- [45] G.E. Boyd, A.W. Adamson, L.S. Meyers, The exchange adsorption of ions from aqueous solutions by organic zeolites: II. Kinetics, *J. Am. Chem. Soc.* 69 (1947) 2836–2848.
- [46] T. Vermeulen, Theory for irreversible and constant pattern solid diffusion, *Ind. Eng. Chem.* 45 (1953) 1664–1670.
- [47] L.D. Michelson, P.D. Gideon, E.G. Pace, L.H. Katal, Removal of soluble mercury from wastewater by complexing techniques. US department of industry: Office of Water Research Technology. Bulletin No. 74. (1975).